

# Implementation and Investigation of a Compact Circular Wide Slot UWB Antenna with Dual Notched Band Characteristics using Stepped Impedance Resonators

Yingsong LI<sup>1</sup>, Wenxing LI<sup>1,2</sup>, Tao JIANG<sup>1,2,3</sup>

<sup>1</sup>College of Inform. and Commun. Engg., Harbin Engineering University, Harbin, Heilongjiang, 150001, P. R. China

<sup>2</sup>Research center of War-ship EMC, Harbin Engineering University, Harbin, Heilongjiang, 150001, P. R. China

<sup>3</sup>Research center of Communication, Harbin Institute of Technology, Harbin, Heilongjiang, 150086, P. R. China

liyingsong@hrbeu.edu.cn, liwenxing@hrbeu.edu.cn, jiangtao@hrbeu.edu.cn

**Abstract.** A coplanar waveguide (CPW) fed ultra-wideband (UWB) antenna with dual notched band characteristics is presented in this paper. The circular wide slot and circular radiation patch are utilized to broaden the impedance bandwidth of the UWB antenna. The dual notched band functions are achieved by employing two stepped impedance resonators (SIRs) which etched on the circular radiation patch and CPW excitation line, respectively. The two notched bands can be controlled by adjusting the dimensions of the two stepped impedance resonators which give tunable notched band functions. The proposed dual notched band UWB antenna has been designed in details and optimized by means of HFSS. Experimental and numerical results show that the proposed antenna with compact size of  $32 \times 24 \text{ mm}^2$ , has an impedance bandwidth ranging from 2.8 GHz to 13.5 GHz for voltage standing-wave ratio (VSWR) less than 2, except the notch bands 5.0 GHz - 6.2 GHz for HIPERLAN/2 and IEEE 802.11a (5.1 GHz - 5.9 GHz) and 8.0 GHz-9.3 GHz for satellite and military applications.

## Keywords

UWB antenna, notch band antenna, stepped impedance resonator, circular wide slot, X-band, SIR.

## 1. Introduction

Since the release of the band 3.1 GHz up to 10.6 GHz by Federal Communications Commission (FCC), ultra-wideband communications systems have been developed widely and rapidly advancing as high data rate, low cost and ultra-low radiation power for short range applications such as wireless personal area network (WPAN) [1]. Because of these advantages of the UWB system, significant researches on UWB antennas have been aroused in academic and industrial fields recently. To meet this requirement, several UWB antennas have been proposed [2]-[5]. However, most of the proposed UWB antennas have either large size owing to the use of a big ground plane or com-

plex structure. Although the ground planes can be miniaturized as reported in [3], they are still not suitable for integration with a printed circuit board. In order to satisfy the integration with microwave printed circuit with small size, printed wide slot antennas which are easily integrated with radio front-end are a good candidate for UWB applications [6]-[7]. So far, microstrip fed UWB antennas [7], rectangular wide slot [8], circular wide slot [9] and hexagonal wide slot [10] UWB antennas have been investigated. However, the designed UWB antennas have large size and cannot cover the whole band ranging from 3.1 GHz to 10.6 GHz. In addition, there are some narrow bands which have been used for a long time in UWB band, such as HIPERLAN/2 bands (5.15 - 5.35GHz and 5.470 - 5.725GHz in Europe) and the IEEE 802.11a bands (5.15 - 5.35GHz and 5.725 - 5.825 GHz in US) for wireless local area network communications, C-band and X band for satellite and military applications. UWB band overlaps with these narrow systems. To reduce or avoid the potential interference between UWB systems and narrow systems, band-stop filters were added at the end of the antennas or devices. So, the cost and the weight of the equipment will increase. Recently, printed UWB antennas with band notch functions have been proposed [11]-[16]. Though these antennas can reduce the interference, many of the proposed notch band antennas suffer from at least one of the following limitations: 1. – a relatively low quality factor (quality factor is the depth of the notch band whose VSWRs are more than 2 in this paper) associate with the notch band, 2. – complex geometry which would be difficult to redesign and the notch band is not tunable, and 3. – the notch bands are obtained by using various slots which deteriorate the radiation patterns. To overcome the shortcoming of the designs, parasitic elements along the printed radiation patch [16] and stubs [17]-[18] were used to design notch band UWB antennas. However, the notch band is also difficult to control. So far, some integrated filters and resonance structures with notch band characteristics have been proposed to reject any undesired bands by using different technologies [19]-[20]. The technologies have been also used to design UWB notch band antennas. M. Ojaroudi et al. have proposed to perturb matching im-

pedance and create an open circuit to form a notch band at the undesired frequency [21]. A most effective technology is to insert open circuited stubs [21]-[22] into the UWB antenna, add dipole-like tuning stubs [17], [20] in the inner of the wide slot, integrate filter [23] in the feed line and active region. And some antennas using SRRs in the fed structures [19], [24] are also utilized to avoid the limited band. All the methods can achieve a good band notch characteristic, but some of the notched band structures are complex and difficult to design. The stepped impedance resonators and the stepped impedance stubs have been used to design notch band UWB filters for a long time [25]-[26].

Based on the previous research above, a CPW-fed circular wide slot ultra-wideband (UWB) antenna with dual notch band characteristics is realized numerically and experimentally. The dual notched band functions are achieved by employing two stepped impedance resonators which etched on the circular radiation patch and CPW excitation line, respectively. One stepped impedance resonator which is used to form the lower notched band is cut on the circular radiation patch. The other stepped impedance resonator which is embedded in the CPW excitation line is to produce the higher notch band. The proposed antenna consists of a circular wide slot structure, a circular radiation patch, two stepped impedance resonators and a 50  $\Omega$  CPW-fed structure. The antenna was successfully optimized using HFSS, fabricated, tested. It was found that the designed antenna satisfied all the requirements in the UWB frequency band except 5.0 - 6.2 GHz for HIPERLAN/2, IEEE 802.11a and C-band applications and 8.0 - 9.3 GHz for X band applications. Details of the antenna design are presented herein, and the measured voltage standing-wave ratio (VSWR), radiation patterns, the gains and group delay are also given. The main contributions in this paper are: 1. dual notch band UWB antenna using SIRs has been proposed and designed in detail; 2. the proposed SIR notch band antenna has been analyzed using SIR theory; 3. the quality factor of the notch band has been improved; 4. The designed antenna has simple notch structure according to the SIR theory which made the proposed dual notch band UWB antenna easy to redesign.

This paper is organized as follows: the geometry structure of the proposed dual notch band UWB antenna will be given in Section 2. The analysis and the discussions of the key parameters are elaborated in Section 3. Section 4 expounds the optimized and the measured results of the proposed UWB antenna with dual notch band characteristic, such as VSWRs and radiation patterns. In Section 5, we will give a conclusion.

## 2. Antenna Design

Fig. 1 illustrates the geometry of the proposed UWB antenna with dual notch band characteristics using two stepped impedance resonators. The proposed dual notch band UWB antenna is printed only on one side of

a substrate with relative permittivity of 2.65, a loss tangent of 0.002 and a thickness of  $h = 1.6$  mm. The size of the antenna is  $32 \times 24 \text{ mm}^2 (L \times W)$ . The dual notch band UWB antenna consists of a circular wide slot structure, a circular radiation patch, two stepped impedance resonators (upper SIR and lower SIR) and a 50  $\Omega$  CPW-fed structure. The 50  $\Omega$  CPW fed structure consists of the CPW excitation line with a width  $W_7 = 3.6$  mm, and the gap between the CPW ground plane and CPW excitation line with width 0.2 mm. The 50  $\Omega$  CPW structure of the proposed UWB antenna is designed using the standard equations [27]. The transmission line model of SIR with stub is shown in Fig. 2. From Fig. 1, the two SIRs with quasi-lumped stubs connected to the central position of the high impedance line. As illustrated in Fig. 2,  $Z_0$  and  $\theta_0$  denote the characteristic impedance and electrical length of the low impedance coupled lines. The high impedance line has the characteristic impedance and electrical length  $Z_s$  and  $\theta_s$ . Meanwhile, the  $Z_i$  and  $\theta_i$  ( $i = 1, 2$ ) show the characteristic impedance and electrical length of the sections of the inner SIR stubs for the stepped impedance resonator etched on the circular radiation patch and designed on the CPW excitation line. The SIR configuration can be analyzed in terms of odd and even excitations. The following resonance frequencies for the odd and even excitations can be separately extracted from condition  $Y_{in} = 0$  [28].

(a) Odd mode resonance condition:  $\tan \theta_0 \tan \theta_s = R$ . (1)

(b) Even mode resonance condition

$$\frac{1}{2R_1} \left[ 1 + \frac{\tan \theta_0 \tan \theta_1}{R} \right] \left[ \frac{\tan \theta_1}{R_1} + \frac{\tan \theta_2}{R_2} \right] + \left[ \tan \theta_s + \frac{\tan \theta_0}{R} \right] \left[ \frac{1}{R_1} + \frac{\tan \theta_1 \tan \theta_2}{R_2} \right] = 0 \quad (2)$$

where the parameters can be described as:

$$R = Z_0 / Z_s,$$

$$R_1 = Z_1 / Z_s, R_2 = Z_2 / Z_s.$$

As expected from Fig. 2 and from (1) and (2), the resonance frequencies for odd mode and even mode can be postulated by using (3) and (4), respectively.

$$f_r \left( \tan \theta_0 + \frac{\tan \theta_s}{R} \right) - \frac{1}{\pi Z_s R} + \frac{\tan \theta_0 \tan \theta_s}{\pi Z_s R^2} = 0, \quad (3)$$

$$\begin{aligned} f_r \left[ 2R_1 \left( \frac{\tan \theta_1 \tan \theta_2}{R_2} - \frac{1}{R_1} \right) (1 - R \tan \theta_s \tan \theta_1) \right. \\ \left. + \left( \frac{\tan \theta_1}{R_1} + \frac{\tan \theta_2}{R_2} \right) (\tan \theta_s + R \tan \theta_0) \right] \\ + \frac{1}{2\pi Z_s} \left( \frac{\tan \theta_1}{R_1} + \frac{\tan \theta_2}{R_2} \right) \left( \frac{\tan \theta_0 \tan \theta_s}{R} - 1 \right) \\ + \frac{R_1}{\pi Z_s} \left( \frac{\tan \theta_1 \tan \theta_2}{R_2} - \frac{1}{R_1} \right) \left( \tan \theta_s + \frac{\tan \theta_0}{R} \right) = 0 \end{aligned} \quad (4)$$

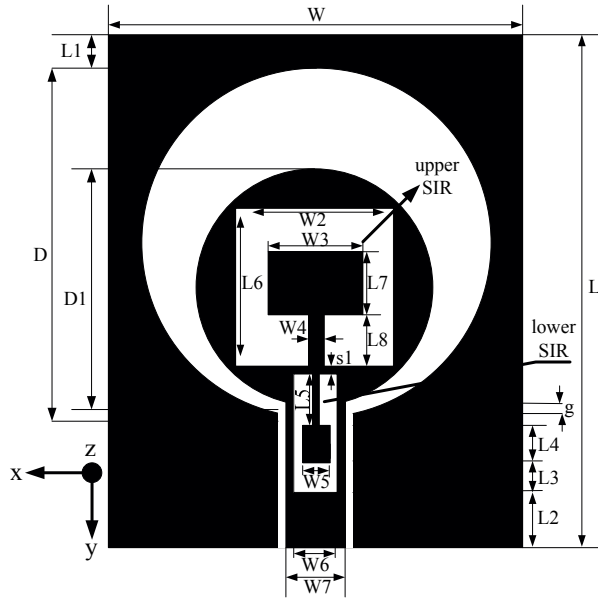


**Fig. 1.** Geometry structure of proposed dual notched band UWB antenna.

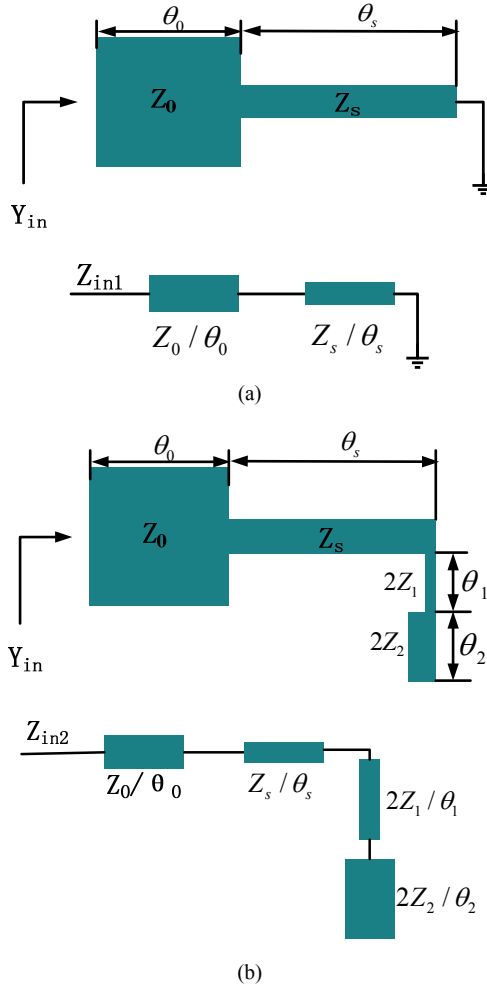


**Fig. 2.** Transmission line model of the symmetrical SIR. (a) Odd resonance model; (b) Even resonance model.

In order to analyze the SIRs which give the notch band functions further, the equivalent circuit of SIR at

resonance frequency has been studied and illustrated in Fig. 3 [28].

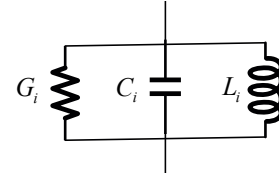


**Fig. 3.** The equivalent circuit of SIR at resonance frequency.

The SIR can also be regarded as a parallel circuit network shown in Fig. 3 where the parameters in the equivalent circuit can be calculated by using  $G_i = b_s/Q_0$ ,  $C_i = b_s/\omega_0$ ,  $L_i = 1/\omega_0 b_s$ . Here,  $Q_0$  is the unloaded- $Q$  of SIR which is determined by physical dimension and the materials of the resonator.  $b_s$  is susceptance slope parameter,  $\omega_0$  is the center frequency at the notch band. The  $Q_0$  and  $b_s$  can be postulated by using the equations in [28] (In the book, the calculation of the equivalent circuit is discussed clearly. So, the calculation formulas are not given here).

Based on the discussions and analysis, the resonance characteristic can be calculated using (1)-(4). Thereby, the dual notch band UWB antenna using SIRs can be easily redesigned according to the SIR theory and the wide slot technology. The center frequency of the notch band can be controlled by adjusting the dimensions of the two SIRs to produce the required notch bands. In this article, we take equations (1)-(4) into consideration to achieve the original dimensions of the SIRs at the beginning of the design and then adjust the dimensions of the geometry for the final design. In addition, the effects of the key parameters of the SIRs are investigated in Section 3. The proposed dual notch band UWB antenna integrates with SIR technology and wide slot which make the antenna easy to redesign.

### 3. Parameters Studies

Every geometrical parameter has different effects on the performance of the proposed dual notch band UWB antenna. In this section, ten parameters of the proposed UWB antenna with dual notched bands using stepped impedance resonators will be described and discussed by using HFSS, respectively: the effect of the length of inner stepped impedance stub of upper SIR L7; the effect of the length of inner stepped impedance stub of upper SIR L8; the effect of the width of the inner stepped impedance stub of upper SIR W3; the effect of the width of the inner stepped impedance stub of upper SIR W4; the effect of the width of the upper SIR W2; the effect of the length of the upper SIR L6; the effect of the length of the inner stepped impedance stub of lower SIR L5; the effect of the width of the inner stepped impedance stub of lower SIR W5; the effect of the length of the inner stepped impedance stub of lower SIR L4; the effect of the width of the lower SIR W6. In the parametric study, one parameter is changed and other parameters are fixed as the optimized parameters which are listed in Tab. 1 in Section 4. In this paper, the

upper SIR produces the lower notch band which is near 5.5 GHz. And the lower SIR generates the higher notch band which is near 9.0 GHz.

### 3.1 The Effect of the Length of the Inner Stepped Impedance Stub of Upper SIR L7

Fig. 4 shows the simulated VSWRs of proposed antenna as a function of frequency for different values of L7. It can be seen from Fig. 4 that the length of stepped impedance stub L7 has an obvious effect on the lower notched band. The center frequency of the lower notched band moves to the lower frequency with the increase of the L7. This is due to the inner stepped impedance stub which changes the resonance frequency of the SIR. The higher notch band also moves to the lower frequency with the increase of L7, and then returns back. This is caused by the two SIRs having the public part which alters the characteristic impedance and electrical length of the high impedance line  $Z_i$  and  $\theta_i$  ( $i = 1, 2$ ). Thereby, the resonance frequencies of the lower and higher notched band have been changed.

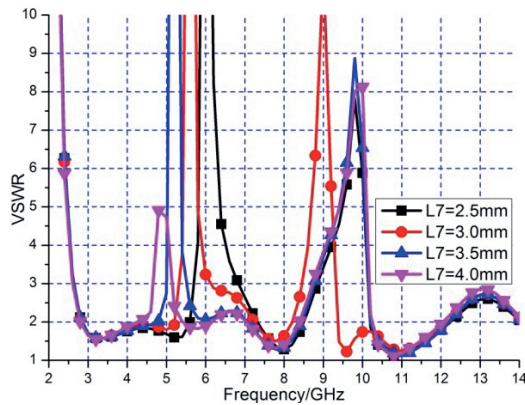


Fig. 4. Effects of L7 on the VSWR.

This can also be verified by (4). At the same time, the quality factors associated with the notch bands are getting worse, which is caused by the changed susceptance slope parameter. Therefore, the dual band notch characteristics can be improved by optimizing the length of inner stepped impedance stub L7.

### 3.2 The Effect of the Length of Inner Stepped Impedance Stub of Upper SIR L8

Fig. 5 gives the simulated VSWR results for proposed dual notched band antenna in terms of L8. With the varying L8 from 1.5 mm to 3.5 mm, the impedance bandwidth and the higher notched band characteristic of the proposed antenna is nearly unchanged. However, the lower notched band moves to the lower band and the quality factor at the lower notch band is deteriorated by increasing the length of L8. In this design, the lower notched band can be tuned from 4.3 GHz to 7.4 GHz in terms of L8. Therefore, the lower notched band can reduce the potential interference between UWB, WLAN, and C band which is used in satel-

ite and military. The various center frequencies of the lower notch band is caused by the inner stepped impedance stub which alters the characteristic impedance and electrical length of the sections of the upper SIR stub  $Z_i$  and  $\theta_i$  ( $i = 1$ ). This will change the  $R_1$ . Therefore, the center resonance frequency of the lower notched band moves to the lower frequency which can be calculated using the equation (4). In addition, the increased length of L8 also changes the coupling between upper SIR and inner stub. The couplings alter the current distributions on inner stub and SIR. This also changes the  $L_i$ ,  $C_i$ . So, the center resonance frequency can be adjusted by choosing proper dimension of the L8 to meet the practical applications.

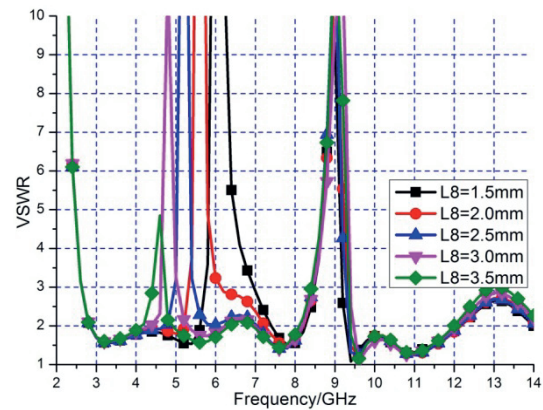


Fig. 5. Effects of L8 on the VSWR.

### 3.3 The Effect of the Width of the Inner Stepped Impedance Stub of Upper SIR W3

Fig. 6 expounds the simulated VSWRs of the proposed antenna as a function of frequency of W3. It is found that the 5.5 GHz notch band frequency moves to the lower frequency with increasing of W3. However, the impedance bandwidth and the higher notch band almost keep invariable. The increased width of the inner stepped impedance stub W3 changes the characteristic impedance and electrical length  $Z_i$  and  $\theta_i$  ( $i = 2$ ). This will change the  $R_2$ . The changed parameters of the inner stepped impedance stub will alter the resonance frequency of lower notch band.

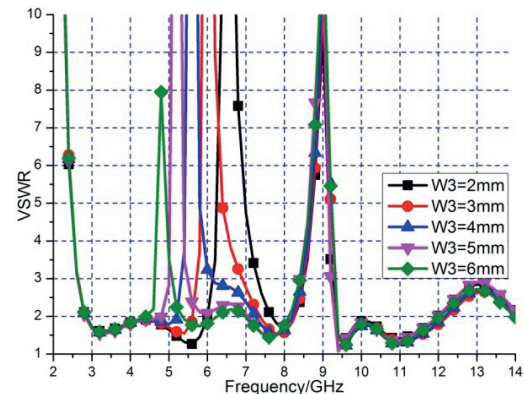


Fig. 6. Effects of W3 on the VSWR.



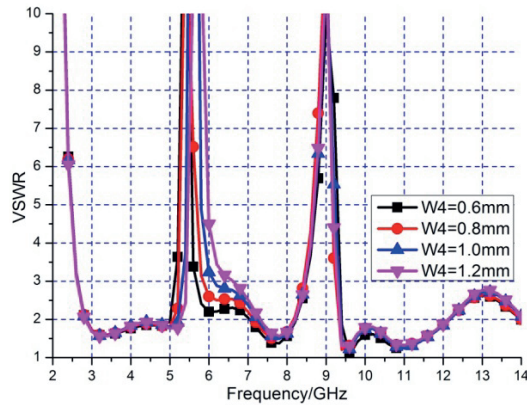


Fig. 7. Effects of W4 on the VSWR.

### 3.4 The Effect of the Width of the Inner Stepped Impedance Stub of Upper SIR W4

Fig. 7 describes the simulated VSWR results for the proposed antenna in terms of W4. The center frequencies of the two notch bands are almost unchanged. However, the increased W4 deteriorates the impedance bandwidth of the dual notched band UWB antenna. In this design, W4 is greater than 0.2 mm for the fabrication process used in our experiment. So, the impedance bandwidth can be adjusted by choosing proper dimension of the W4. In addition, the center frequency of the lower notch band can be tuned slightly to meet WLAN applications.

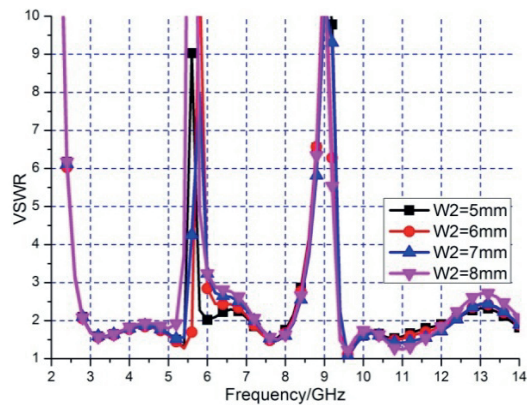


Fig. 8. Effects of W2 on the VSWR.

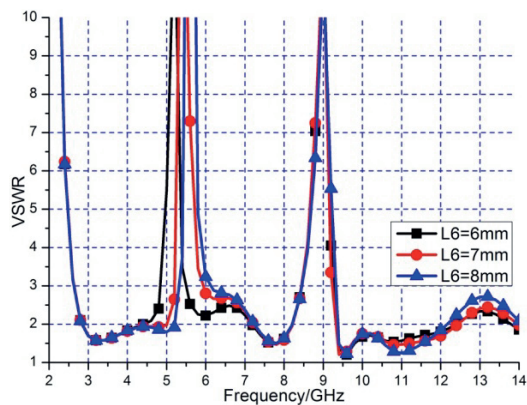


Fig. 9. Effects of L6 on the VSWR.

### 3.5 The Effect of the Width of the Upper SIR W2

In this design, the SIR works at its even excitation. So the upper SIR also has an impact on the center resonance frequency of the lower notch band. It can be seen from Fig. 8 that the center frequency of the lower notch band changed a little. But the quality factor associated with the lower notch band worsened. In the design, the upper SIR is designed first. Then, the inner stepped impedance stub is adjusted to satisfy the requirement of the practical project.

### 3.6 The Effect of the Length of the Upper SIR L6

Fig. 9 demonstrates the simulated VSWR characteristics for different values of L6. From Fig. 9, we can find that L6 has a little effect on the center frequency of the lower notch band. Because the SIRs work on its even excitation which can be adjusted not only using inner stepped impedance stub but also using the high impedance lines of the SIRs [28]. The various L6 can change the characteristic impedance and electrical length  $Z_0$ ,  $\theta_0$ ,  $Z_s$  and  $\theta_s$  of the upper SIR. Therefore, at the beginning of the design, we first take the SIR parameters into consideration to calculate the resonance frequency.

### 3.7 The Effect of the Length of the Inner Stepped Impedance Stub of Lower SIR L5

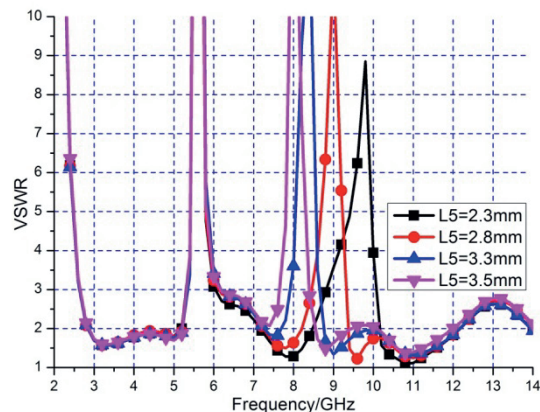


Fig. 10. Effects of L5 on the VSWR.

Fig. 10 elaborates the simulated VSWRs against the frequency for different values of L5. It can be seen from Fig. 10 that the length of the inner stepped impedance stub of lower SIR L5 has an obvious effect on the center frequency of the higher notch band of the proposed dual notch band UWB antenna. The increased length L5 alters the characteristic impedance and electrical length of the inner SIR stub  $Z_i$  and  $\theta_i$  ( $i = 1$ ). This will change  $R_1$  of the lower SIR. This can also be postulated by using the equations (2) and (4). The resonance characteristic and the parameters of the lower SIR are similar to the upper SIR. In addition, the lower SIR embedded in the CPW excitation line disturbs the current distributions of the proposed antenna effec-

tively. In this design, the higher notch band is designed in the X-band which is widely used in deep space communication according to the practical project. So, at the beginning of the design, the lower SIR is calculated using the SIR theory and equations (1)-(4) to meet the requirement of our practical project. The quality factor associated with the higher notch band can be adjusted by the increase of the length  $L_5$ .

### 3.8 The Effect of the Width of the Inner Stepped Impedance Stub of Lower SIR W5

Fig. 11 illustrates the simulated VSWRs with width varying from 0.8 mm to 1.6 mm. It can be seen from Fig. 11 that the center frequency of the higher notch band moves to the lower frequency. The quality factor of higher notch band has obviously been improved. This is caused by the altered dimension of  $W_5$  which not only influences the resonance frequency of the lower SIR but also changes distribution capacity. Therefore, during the optimization, we take the discussions of the upper SIR into consideration to obtain the proper dimensions of the lower SIR.

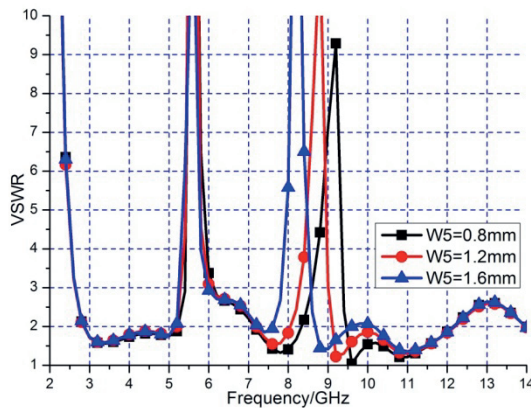


Fig. 11. Effects of  $W_5$  on the VSWR.

### 3.9 The Effect of the Length of the Inner Stepped Impedance Stub of Lower SIR L4

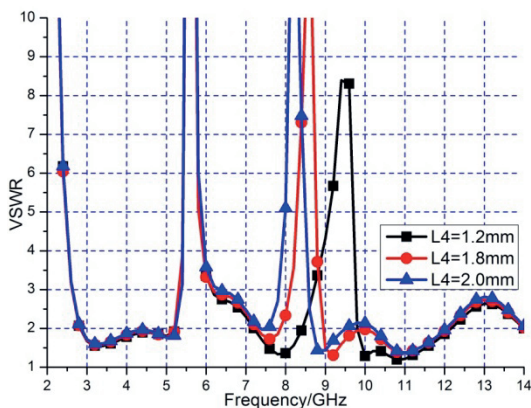


Fig. 12. Effects of  $L_4$  on the VSWR.

Fig. 12 describes the simulated VSWRs with varying  $L_4$ . It can be seen from Fig. 12 that the center frequency of the higher notch band moves to the low frequency with the increasing length of  $L_4$ . At the same time, the quality factor of higher notch band has also been improved. The varied length also alters the characteristic impedance and electrical  $Z_i$  and  $\theta_i$  which have been discussed in the explanation of the upper SIR. Thereby, the resonance characteristic of higher notched band can be optimized according to the argumentation of the upper SIR. This can also be verified by (4).

### 3.10 The Effect of the Width of the Lower SIR W6

Fig. 13 gives the simulation of the VSWRs of various  $W_6$ . From Fig. 13, the center frequency of the two notch bands is almost constant. But the quality factor of higher notch band is improved. In our design, the designed width  $W_6$  is less than 3 mm according to the width of the CPW excitation line. Thereby, at the beginning of the design of the two stop bands, all the parameters of the SIRs and the dimensions of the two inner stepped impedance stubs are taken into consideration to generate the required resonance frequencies.

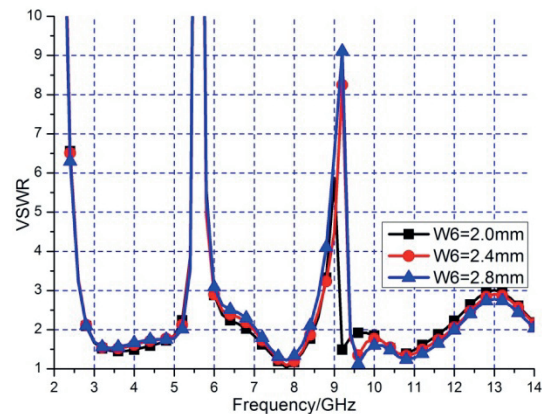


Fig. 13. Effects of  $W_6$  on the VSWR.

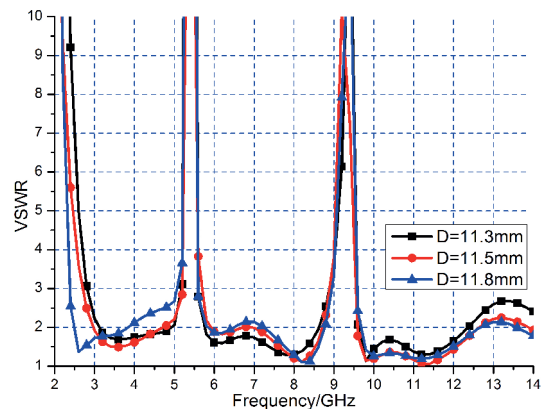


Fig. 14. Effects of  $D$  on the VSWR.

Besides the discussions above, the parameters of the circular wide slot  $D$ , the gap  $g$  between the circular

radiation patch and the CPW ground plane, and the circular radiation patch D1 have also been investigated. The simulated results are shown in Fig. 14, Fig. 15 and Fig. 16. We can see from Fig. 14 that the impedance bandwidth of proposed UWB antenna is getting narrower by increasing D. This is caused by the reduced coupling between wide slot and radiation patch.

Fig. 15 shows the simulated VSWRs with varying D1. It can be seen from Fig. 15 that the impedance bandwidth is getting better by increase of D1. However, the bandwidth of higher notch band is getting narrower. This is due to the increased D1 which changes the coupling between the wide slot and the radiation patch. This will change the distributed inductance and capacity of the circular wide slot. So, the impedance bandwidth and the bandwidth of the notch band can be adjusted according to the practical requirement.

Fig. 16 shows the effects of gap g. The impedance bandwidth can also be controlled by adjusting the gap g. With the increase of gap g, the impedance bandwidth has a little deteriorated. In addition, the bandwidth of the two impedance bandwidth of the proposed antenna can be broadened by the proper choice of the parameters of D, D1 and g.

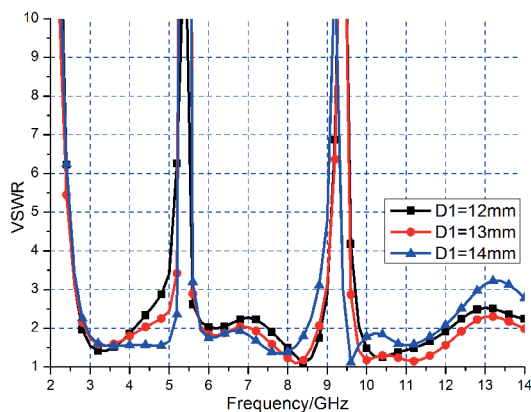


Fig. 15. Effects of D1 on the VSWR.

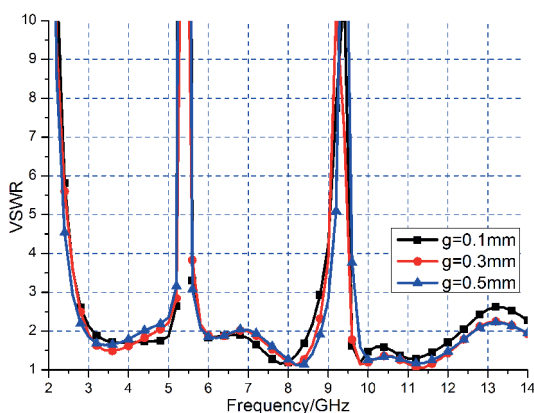


Fig. 16. Effects of gap g on the VSWR.

Based on the discussions of the key parameters of the SIRs and wide slot, we can see that the lower notch band

can be tuned from 4.0 GHz to 7.7 GHz with the VSWR > 10. The higher notch band can be tuned from 7.2 GHz to 10.3 GHz with VSWR > 8. The proposed two notch bands can be tuned by adjusting the dimensions of the SIRs and stubs to meet the practical applications. The proposed antenna has simple structure and can be re-designed easily according to the SIR theory and wide slot antenna technology.

In order to investigate the proposed dual notch band UWB antenna further, the current distributions of the proposed antenna are investigated by using the Ansoft high frequency structure simulator (HFSS) based on Finite Element Method (FEM). The current distributions of the proposed dual notch band antenna at 3.5 GHz, 5.5 GHz, 7 GHz, 9 GHz and 10.5 GHz are shown in Fig. 16(a), Fig. 17(b), Fig. 17(c), Fig. 17(d), Fig. 17(e), respectively. The current distributions of the proposed UWB antenna with only upper SIR at 5.5 GHz and without the two SIRs at 5.5 GHz and 9 GHz are also shown in Fig. 17(f), Fig. 17(g), Fig. 17(h), respectively.

Fig. 17(a) shows the current distributions at 3.5 GHz of the proposed dual notch band UWB antenna. The current flows along the CPW excitation line and the edge of the circular wide slot. The current distributions along the circular radiation patch and the two SIRs are small. Fig. 17(b) gives the current distributions at 5.5 GHz of the proposed antenna with two notch bands. The current mainly flows along the upper SIR and its inner stepped impedance stub which produces a resonance frequency of lower notch band at 5.5 GHz. The current distributions along CPW ground plane are small. Fig. 17(c) shows the current distributions of the proposed dual notch band UWB antenna at 7.0 GHz. The current mainly flows along the CPW excitation line and the edge of the circular radiation patch, while the current distributions at the two SIRs are small. Fig. 17(d) illustrates the current distributions of the proposed UWB antenna with two SIRs at 9.0 GHz. It can be seen from Fig. 17(d) that the current distributions at the CPW excitation line and the lower SIR are large. So, the higher notch band near 9.0 GHz is generated by the lower SIR. Fig. 17(e) gives the current distributions of the proposed dual notch band UWB antenna at 10.5 GHz. From Fig. 17(e), we can see that the current mainly flows along the CPW excitation line and the edge of the gap between (a) UWB antenna at 3.5 GHz with two SIRs; (b) UWB antenna at 5.5 GHz with two SIRs; (c) UWB antenna at 7.0 GHz with two SIRs; (d) UWB antenna at 9.0 GHz with two SIRs; (e) UWB antenna at 10.5 GHz with two SIRs; (f) UWB antenna at 5.5 GHz with upper SIR; (g) UWB antenna at 5.5 GHz w/o two SIRs; (h) UWB antenna at 9.0 GHz w/o two SIRs the circular radiation patch and the CPW ground plane. The current distributions at the two SIRs are small. Fig. 17(f) shows the current distributions of the proposed UWB antenna with only upper SIR at 5.5 GHz. We can see from Fig. 17(f), the current distributions mainly spread along the SIR and its inner stepped impedance stub. So, a notch band is generated near



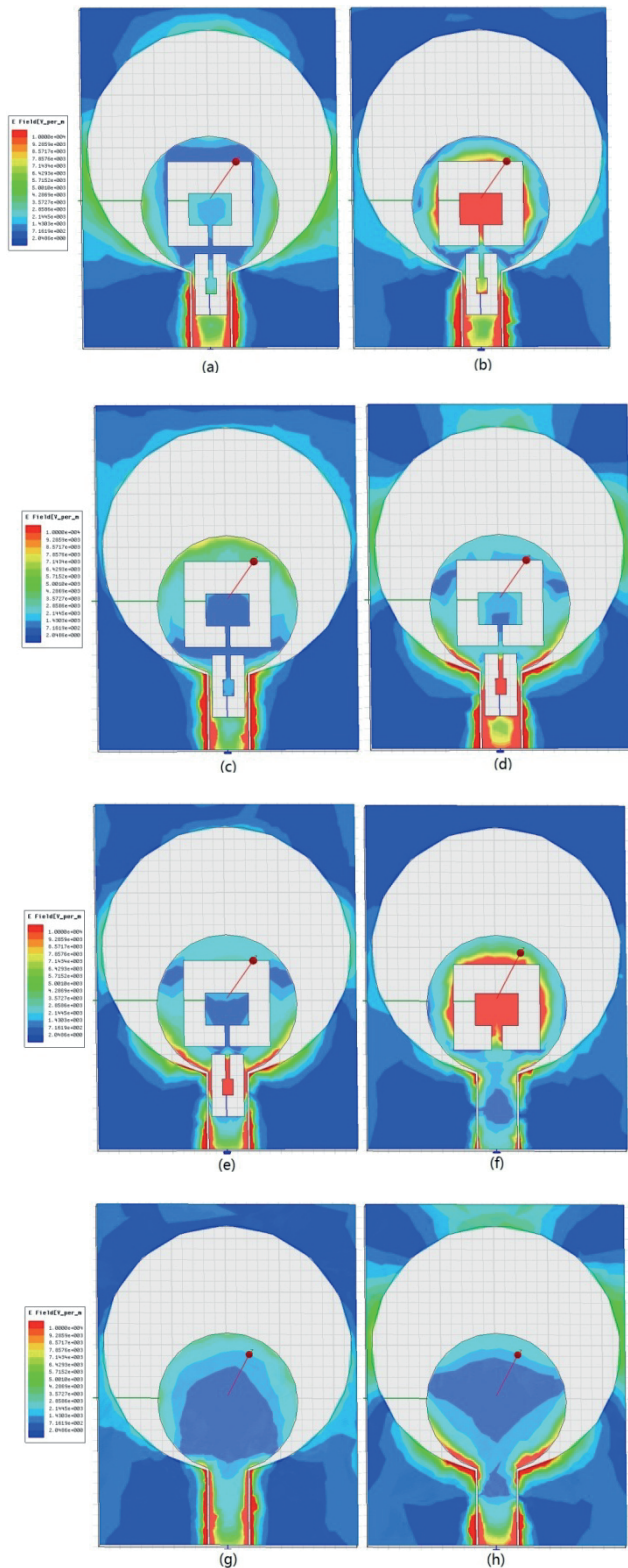


Fig. 17. Current distributions of the proposed antenna.

5.5 GHz. The current distributions at CPW ground plane and the CPW excitation line are small. Fig. 17(g) describes the current distributions of the proposed UWB antenna without the two SIRs at 5.5 GHz. From Fig. 17(g), we can see that the current mainly flows along the CPW excitation line and the edge of the circular radiation patch. The current distributions in the CPW ground plane are tiny.

Fig. 17(h) illustrates the current distributions of the proposed UWB antenna without the two SIRs at 9.0 GHz. It can be seen from Fig. 17(h) that the current mainly flows along the CPW excitation line and the edge of the gap between the circular radiation patch and the CPW ground plane. From the current distributions discussed above, it is found that the dual notch band characteristics are obtained using the upper SIR and lower SIR which give the 5.5 GHz notch band and 9.0 GHz notch band, respectively.



Fig. 18. Photograph of the antenna.

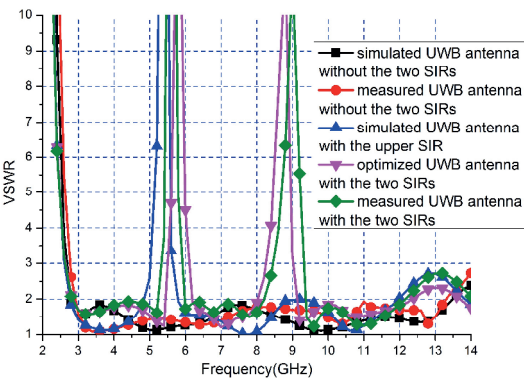


Fig. 19. VSWRs of the proposed antenna.

4. Results and Discussions

According to the study and the discussions of the key parameters, the proposed dual notch band UWB antenna has been optimized by utilizing HFSS. During the optimizing process, the parameters are adjusted according to the results of the parametric study and the current distributions discussed above. The optimized results are listed in Tab. 1.

Parameter	Value	Parameter	Value
W	24	L	32
D	23.2	D1	13
W2	8	L6	8
L1	1.9	L7	3
W3	4	L8	2
W4	1	W5	1.4
W6	3	g	0.2
L2	3	L3	1.5
L4	1.5	L5	2.5
W7	3.6	s1	0.7

Tab. 1. Parameters of the proposed antenna (Unit: mm).

To evaluate the performance of the optimized UWB antenna, the proposed antenna is fabricated and tested. The measured VSWRs of the antenna are obtained by using Anritsu 37347D vector network analyzer. In order to compare the simulated and measured results of the proposed dual notch band UWB antenna with two SIRs, the proposed antenna with only upper SIR and without the two SIRs are also investigated herein. A photograph of the proposed antenna is shown in Fig. 18 and the VSWRs of the antennas are shown in Fig. 19.

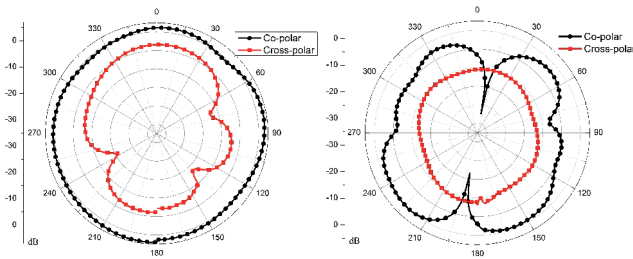


Fig. 20. Radiation patterns 3.5 GHz.

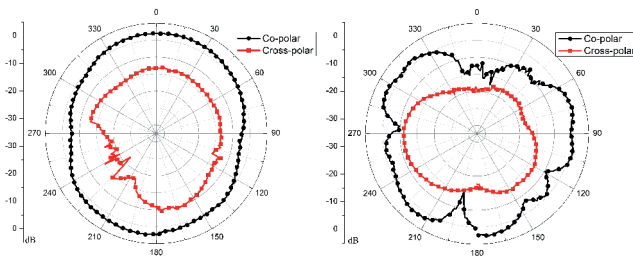


Fig. 21. Radiation patterns 7.0 GHz.

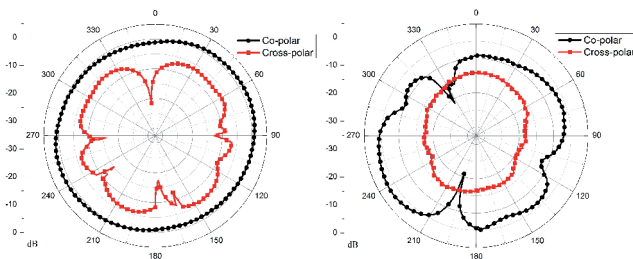


Fig. 22. Radiation patterns 10.5 GHz.

From Fig. 19, the measured results agree well with the simulated results which help to verify the accuracy of the simulation. The differences between the simulated and measured values may be due to the errors of the manufactured antenna and the SMA connector to CPW-fed transition, which is included in the measurements but not taken into account in the calculated results. It can also find that the two notch bands are obtained by using the two SIRs. The notch band near 5.5 GHz is produced by the upper SIR and the 9 GHz notch band is provided by the lower SIR. This is consistent with the simulated and analyzed current distributions. The proposed antenna without the two SIRs has an impedance bandwidth of 131 % according to the center frequency of the UWB antenna. It also can be seen from Fig. 19 that the proposed dual notch band has better quality factor than most of the previous proposed notch band UWB antennas.

The measured radiation patterns at 3.5 GHz, 7.0 GHz and 10.5 GHz are shown in Fig. 20, Fig. 21 and Fig. 22, respectively. The left is the H-plane and the right is E-plane. The proposed UWB antenna has a nearly omnidirectional characteristic in the H-plane and quasi omnidirectional pattern in the E-plane. In this design, xz plane is H-plane ( $\phi = 0^\circ$ ) and yz-plane is E-plane ( $\phi = 90^\circ$ ) for the proposed antenna. The radiation patterns in the E-plane deteriorate more or less with the increasing of frequency, but the radiation patterns are still nearly quasi omnidirectional. In some frequencies and in some directions, the co-polar and cross-polar levels are quite close. This is caused by the electromagnetic leak of the etched SIR filters which have some influence on the radiation patterns. The co-polar and cross-polar levels in fixed frequency of E- and H-planes in some directions are different. However, the proposed antenna can be also used as a dual notch band UWB antenna compared the previous UWB antennas.

The peak gains of the proposed antenna at these frequencies are achieved by comparing to a double ridged horn antenna. At each frequency, we find the maximum level of radiation pattern to measure the gains and the space loss is also considered in the measurement. A stable gain can be obtained throughout the operation band except the two notched frequencies. In order to compare, the proposed antenna without the two SIRs is also measured. The peak gains of the proposed antennas with and without the two SIRs are shown in Fig. 23. The measured gain of the proposed antenna without two SIRs is increased from 1.86 dBi to nearly 5.1 dBi which is caused by the deteriorated radiation patterns of the proposed antenna at the high band. In the operation band, the proposed UWB antenna without the two SIRs has stable gains with fluctuation less than 3.3 dBi. But the gain of the proposed antenna with the two SIRs dropped quickly from 5.0 GHz to 6.2 GHz and from 8 GHz to 9.3 GHz. As desired, two sharp gains decreased in the vicinity of 5.5 GHz and 9 GHz. The gains drop deeply to -5.2 dBi at the lower notch band and -4.2 dBi at the higher notch band. From Fig. 23, the notch gains have a little better than most of the previous proposed notch band UWB antennas. This is caused by the improved quality factor characteristics discussed in Section 3. In the future, we will develop novel notch band UWB antenna to improve the notch gains further.

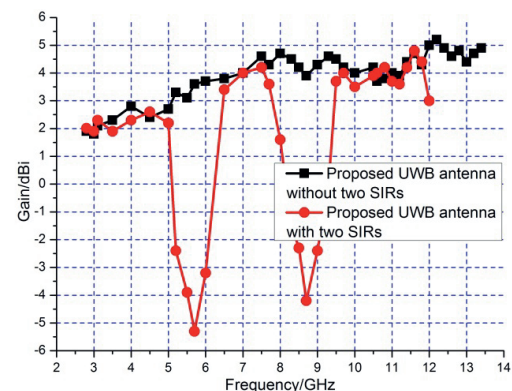


Fig. 23. Measured gain of the proposed UWB antenna.



Fig. 24 shows the variation of the group delay. The group delay is within 2.0 ns in the UWB band, except the two notch bands where the maximum group delay is nearly 9 ns and 7 ns at the 5.5 GHz and 9 GHz notch band, respectively.

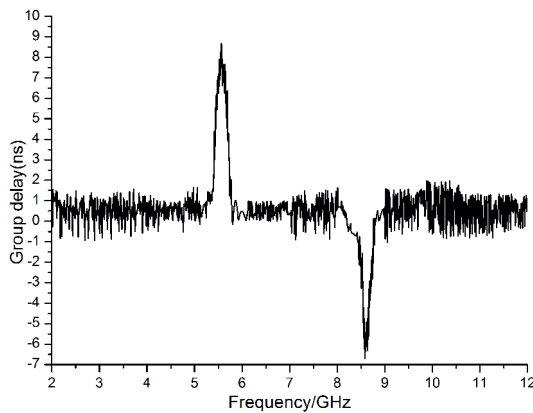


Fig. 24. Simulated group delay.

## 5. Conclusion

A CPW-fed circular wide slot UWB antenna with dual band-notch characteristics is proposed numerically and experimentally. The two notch bands are obtained by using two SIRs which etched in the circular radiation patch and embedded in the CPW excitation line, respectively. The dual notch bands can reduce the potential interference between UWB and WLAN, X-band. And the antenna has a small size of  $32 \times 24 \times 1.6 \text{ mm}^3$ . The proposed UWB antenna without the two SIRs has an impedance bandwidth over 10.7 GHz. The dual notch band with the two SIRs has been analyzed and investigated by means of HFSS. The current distributions of the proposed dual band notch antenna, the proposed antenna with only upper SIR and the antenna without the two SIRs are also discussed in this paper. The antenna is successfully designed, optimized, fabricated and tested. The results show that the antenna not only has good dual notch band characteristic but also has large impedance bandwidth and good radiation patterns.

## Acknowledgements

This work was supported by a grant from the National Defense “973” Basic Research Development Program of China (No.6131380101). This paper is also supported by the National Nature Science Fund of China (No.60902014), Nature Science Fund of Heilongjiang (QC2009C66). The authors are also thankful to Hebei VSTE Science and Technology Co., Ltd. for providing the measuring facility. The authors are indebted to the editor and to the two anonymous reviewers who gave us many helpful comments and constructive suggestion to improve this paper.

## References

- [1] Federal communications commission. *First order and report, Revision of Part 15 of commission's rules regarding UWB transmission systems*, FCC 02-48. 2002.
- [2] KIM, J. I., JEE, Y. Design of ultrawideband coplanar waveguide-fed LI-shape planar monopole antennas. *IEEE Antennas and Wireless Propagation Letters*, 2007, vol. 6, p. 383 - 387.
- [3] ČERNÝ, P., MAZÁNEK, M. Optimization of transient response radiation of printed ultra wideband dipole antennas (using particle swarm optimization method). *Radioengineering*, 2007, vol. 16, no. 2, p. 9 - 14.
- [4] RAZAVI-RAD, M., GHOBADI, C., NOURINIA, J., ZAKER, R. A small printed ultra-wideband polygon-like wide-slot antenna with a fork-like stub. *Microwave Journal*, 2010, vol. 53, no. 3, p. 118 - 126.
- [5] LIN, C. C., CHUANG, H. R. A 3 - 12 GHz UWB planar triangular monopole antenna with ridged ground-plane. *Progress In Electromagnetics Research*, 2008, vol. 83, p. 307 - 321.
- [6] HABIB, M. A., DENIDNI, T. A. Design of a new wideband microstrip-fed circular slot antenna. *Microwave and Optical Technology Letters*, 2006, vol. 48, no. 5, p. 919 - 923.
- [7] LIANG, J., GUO, L., CHIAU, C. C., CHEN, X., PARINI, C. G. Study of CPW-fed circular disc monopole antenna for ultra wideband applications. *IEE Proceedings Microwaves, Antennas and Propagation*, 2005, vol. 152, no. 6, p. 520 - 526.
- [8] LI, Y. S., YANG, X. D., LIU, C. Y., JIANG, T. Compact CPW-fed ultra-wideband antenna with dual band-notched characteristics. *Electronics Letters*, 2010, vol. 46, no. 14, p. 967 - 968.
- [9] PAN, C. J., LEE, C., HUANG, C. Y., LIN, H. C. Band notched ultra-wideband slot antenna. *Microwave and Optical Technology Letters*, 2006, vol. 48, no. 12, p. 2444 - 2446.
- [10] YE, L. H., CHU, Q. X. 3.5/5.5 GHz dual band notch ultra-wideband slot antenna with compact size. *Electronics Letters*, 2010, vol. 46, no. 5, p. 325 - 327.
- [11] BAHADORI, K., RAHMAT-SAMII, Y. A miniaturized elliptic-card UWB antenna with WLAN band rejection for wireless communications. *IEEE Transactions on Antennas and Propagation*, 2007, vol. 55, no. 11, p. 3326 - 3332.
- [12] YU, F., WANG, C. H. A CPW-Fed Novel planar ultra-wideband antenna with a band-notch characteristic. *Radioengineering*, 2009, vol. 18, no. 4, p. 551 - 555.
- [13] AZARMANESH, M., SOLTANI, S., LOTFI, P. Design of an ultra-wideband monopole antenna with WiMAX, C and wireless local area network. *IET Microwaves, Antennas & Propagation*, 2011, vol. 5, no. 6, p. 728 - 733.
- [14] LI, Y. S., YNAG, X. D., YANG, Q., LIU, C. Y. Compact coplanar waveguide fed ultra wideband antenna with a notch band characteristic. *AEU - International Journal of Electronics and Communications*, 2011, vol. 65, no. 11, p. 961 - 966.
- [15] VUONG, T. P., GHIOTTO, A., DUROC, Y., TEDJINI, S. Design and characteristics of a small U-slotted planar antenna for IR-UWB. *Microwave and Optical Technology Letters*, 2007, vol. 49, no. 7, p. 1727 - 1731.
- [16] JUNG, J., LEE, H., LIM, Y. Compact band-notched ultra-wideband antenna with parasitic elements. *Electronics Letters*, 2008, vol. 44, no. 19, p. 1104 - 1106.
- [17] LI, Y. S., YANG, X. D., LIU, C. Y., JIANG, T. Analysis and investigation of a cantor set fractal UWB antenna with a notch-

- band characteristic. *Progress In Electromagnetics Research B*, 2011, vol. 33, p. 99 - 114.
- [18] ABDOLLAHVAND, M., DADASHZADEH, G., MOSTAFA, D. Compact dual band-notched printed monopole antenna for UWB application. *IEEE Antenna and Wireless Propagation Letters*, 2010, vol. 9, p. 1148 - 1151.
  - [19] TANG, M. C., XIAO, S. Q., DENG, T. W., WANG, D., GUAN, J., WANG, B. Z., GE, G. D. Compact UWB antenna with multiple band-notches for WiMAX and WLAN. *IEEE Transactions on Antennas and Propagation*, 2011, vol. 59, no. 4, p. 1372 - 1376.
  - [20] LEE, J. N., PARK, J. K., CHOI, II H. A compact filter-combined ultra-wide band antenna for UWB applications. *Microwave and optical Technology Letters*, 2008, vol. 50, no. 11, p. 2839-2845.
  - [21] OJAROUDI, M., GHANBARI, G., OJAROUDI, N., GHOBADI, C. Small square monopole antenna for UWB applications with variable frequency band-notch function. *IEEE Antenna and Wireless Propagation Letters*, 2009, vol. 8, p. 1061-1064.
  - [22] LIU, H. W., KU, C. H., WANG, T. S., YANG, C. F. Compact monopole antenna with band-notched characteristic for UWB applications. *IEEE Antenna and Wireless Propagation Letters*, 2010, vol. 9, p. 397 - 400.
  - [23] DJAIZ, A., NEDIL, M., HABIB, M. A., DENIDNI, T. A. Design of a new UWB integrated antenna filter with a rejected WLAN band at 5.8 GHz. *Microwave and Optical Technology Letters*, 2011, vol. 53, no. 6, p. 1298 - 1302.
  - [24] CHANG, T.-N., WU, M.-C. Band notched design for UWB antennas. *IEEE Antennas and Wireless Propagation Letters*, 2008, vol. 7, p. 636 - 640.
  - [25] KIM, C. H., CHANG, K. Ring resonator bandpass filter with switchable bandwidth using stepped impedance stubs. *IEEE Transactions on Microwave Theory and Techniques*, 2010, vol. 58, no. 12, p. 3936 - 3944.
  - [26] LIU, C. Y., JIANG, T., LI, Y. S. A novel UWB filter with notch-band characteristic using radial-UIR/SIR loaded stub resonators. *Journal of Electromagnetic Waves and Applications*, 2011, vol. 25, p. 233 - 245.
  - [27] GARG, R., BHARTIA, P., BAHL, I., ITTIPIBOON, A. *Microstrip Antenna Design Hand Book*. Norwood (MA, USA): Artech House, 2001.
  - [28] MAKIMOTO, M., YAMASHITA, S. *Microwave Resonators and Filters for Wireless Communication: Theory, Design and Application*. Berlin (Germany): Springer, 2001.

## About Authors ...

**Yingsong LI** was born in Henan, China, 1982. He received his B.S. degree in Electrical and Information Engineering in 2006, the M.S. degree in Electromagnetic Field and Microwave Technology from Harbin Engineering University, China. Now he is a Ph.D. Candidate in Harbin Engineering University, China. He is a student member of Chinese Institute of Electronics (CIA), IEEE and IEICE. His recent research interests are mainly in microwave theory, small antenna technologies, microwave and millimeter wave circuits.

**Wenxing LI** received the B.S. and M.S. degrees in from Harbin Engineering University, Harbin, Heilongjiang, China, in 1982 and 1985, respectively. He is currently a full professor of College of Information and Communication Engineering, Harbin Engineering University, China. He is also the head of Research Centre of EM Engineering & RF Technology. He visited the Department of Electrical Engineering, The Pennsylvania State University, USA from June to August 2010. He also visited Oriental Institute of Technology, Taiwan from August to October, 2010. His recent research interests are mainly in computational electromagnetic, microwave engineering, modern antenna design and microwave and millimeter wave circuits. He is also the section chair of the 30<sup>th</sup> Progress in Electromagnetics Research Symposium (PIERS) and TPC of IEEE International Workshop on Electromagnetics (iWEM).

**Tao JIANG** was born in Heilongjiang, China, in 1973. He received his B.S. degree of Electrics Engineering in 1994, the M.S. degree of Information & Signal Processing in 1999 and the Ph.D. degree of Communication & Information System in 2002 from Harbin Engineering University, China respectively. He worked in Harbin Institute of Technology, China as a postdoc in 2003 and worked in National University of Singapore as a research fellow in 2004. Now he is a professor in Harbin Engineering University, China. He is a member of IEEE. His recent research interests are mainly in computational electromagnetic, microwave engineering, microwave propagation & navigation and EMC.